

Unexpected Disproportionation Mechanism for Proton-Transfer Reactions between 17-Electron Metal Hydride Cation Radicals and Neutral 18-Electron Metal Hydrides

Kjell-Tore Smith, Christian Rømming, and Mats Tilset*

Contribution from the Department of Chemistry, University of Oslo, P.O. Box 1033 Blindern, N-0315 Oslo, Norway

Received April 9, 1993*

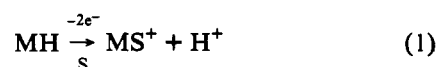
Abstract: The hydrides CpRu(PR₃)₂H ((PR₃)₂ = (PPh₃)₂, **1**; dpmp, **2**; dppe, **3**; and dppp, **4**) undergo one-electron oxidations at -0.1 to -0.3 V vs Cp₂Fe/Cp₂Fe⁺. The oxidations of **1** and **4** are nearly chemically reversible in acetonitrile; in THF, the oxidation of **3** also exhibits partial chemical reversibility. Chemical oxidation of **1-4** in acetonitrile yields 1:1 mixtures of CpRu(PR₃)₂(NCMe)⁺ and the dihydride or dihydrogen complexes CpRu(PR₃)₂H₂⁺, indicative of proton transfer from the hydride cation radicals to the neutral hydrides. A detailed kinetic and mechanistic investigation of the reactions of **1**^{•+} and **4**^{•+} was performed by derivative cyclic voltammetry. Kinetic data are in accord with a disproportionation mechanism. The disproportionation is facilitated by acetonitrile coordination at the 17-electron cation radicals and is followed by proton transfer from highly acidic dications, rather than from the less acidic cation radicals, of the substrates. By the use of a thermochemical cycle that combines the electrode potentials for **2** and **3** and the pK_a data for the corresponding dihydrogen complexes, it is found that H₂ is activated by ca. 100 kJ/mol toward homolysis when coordinated at the Ru centers. The structure of **1** was determined by X-ray crystallography. Crystal data for **1**: triclinic space group, P $\bar{1}$, Z = 2, a = 9.736(1) Å, b = 10.117(1) Å, c = 17.659(3) Å, α = 90.91(1)°, β = 105.93(1)°, γ = 99.19(1)°, R = 0.041, R_w = 0.047.

Introduction

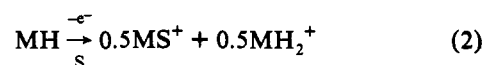
Reactions that involve cleavage or formation of metal-hydrogen bonds are of crucial importance in catalysis and stoichiometric processes.¹ A considerable amount of data has been accumulated concerning the thermodynamics of M-H heterolysis (H⁺ dissociation)² and homolysis (H[•] dissociation)^{1b,2a,p,3} of coordinatively saturated species. The kinetics of transfer of protons^{1b,2a,4} and hydrogen atoms^{1b,2a,5} from saturated metal centers have also been addressed, although to a lesser extent. The proton-transfer reactions are relatively slow processes, reflecting the need for structural and electronic reorganization during the proton transfer.

The oxidation of neutral 18-electron metal hydrides serves to activate the M-H bonds toward deprotonation^{2p,6} and homol-

ysis.^{2p,6e} The homolytic activation amounts to only ca. 30 kJ/mol,^{2p,6e} while the acidity enhancement is about 20 pK_a units^{2p,6a,b,e} or more, or greater than 150 kJ/mol for a number of hydrides. Reactions that appear to involve proton transfer from metal hydride cation radicals MH^{•+} are commonly observed. Cation radicals of neutral hydrides that are already rather acidic undergo spontaneous deprotonation reactions in which the medium (solvent/electrolyte) acts as the proton acceptor.^{6a} These oxidation reactions constitute overall two-electron processes (eq 1).



In other cases, the neutral parent hydride is the strongest base present and acts as the proton acceptor. A cationic dihydride^{6a,d} or dihydrogen^{6b,c,f,j} complex, MH₂⁺, then results from an overall one-electron oxidation (eq 2; S = solvent). The primary product



of the deprotonation, the radical M[•], usually undergoes a second oxidation to generate the solvate MS⁺.

During an investigation of the oxidation chemistry of CpRu(PPh₃)₂H in dichloromethane, we noted that the proton transfer from CpRu(PPh₃)₂H^{•+} was rather slow, as evidenced by a nearly reversible cyclic voltammogram obtained even at a voltage sweep rate, ν, as low as 0.1 V/s.^{6d} Furthermore, the extent of chemical reversibility that was seen in cyclic voltammograms of this compound was concentration dependent, high substrate

* Abstract published in *Advance ACS Abstracts*, September 1, 1993.

(1) (a) *Transition Metal Hydrides: Recent Advances in Theory and Experiment*; Dedieu, A., Ed.; VCH Publishers: New York, 1991. (b) Bullock, R. M. *Comments Inorg. Chem.* **1991**, *12*, 1. (c) Collman, J. P.; Hegedus, L. S.; Norton, J. R.; Finke, R. G. *Principles and Applications of Organotransition Metal Chemistry*; University Science Books: Mill Valley, CA, 1987. (d) Parshall, G. W. *Homogeneous Catalysis*; Wiley: New York, 1979.

(2) (a) Kristjánssdóttir, S. S.; Norton, J. R. In ref 1a. (b) Pearson, R. G. *Chem. Rev.* **1985**, *85*, 41. (c) Jordan, R. F.; Norton, J. R. *J. Am. Chem. Soc.* **1982**, *104*, 1255. (d) Moore, E. J.; Sullivan, J. M.; Norton, J. R. *J. Am. Chem. Soc.* **1986**, *108*, 2257. (e) Kristjánssdóttir, S. S.; Moody, A. E.; Weberg, R. T.; Norton, J. R. *Organometallics* **1988**, *7*, 1983. (f) Kristjánssdóttir, S. S.; Loendorf, A. J.; Norton, J. R. *Inorg. Chem.* **1991**, *30*, 4470. (g) Jia, G.; Morris, R. H. *J. Am. Chem. Soc.* **1991**, *113*, 875. (h) Morris, R. H. *Inorg. Chem.* **1992**, *31*, 1471. (i) Jia, G.; Lough, A. J.; Morris, R. H. *Organometallics* **1992**, *11*, 161. (j) Chinn, M. S.; Heinekey, D. M. *J. Am. Chem. Soc.* **1990**, *112*, 5166. (k) Sowa, J. R., Jr.; Zanotti, V.; Angelici, R. J. *Inorg. Chem.* **1991**, *30*, 4108. (l) Sowa, J. R., Jr.; Zanotti, V.; Facchin, G.; Angelici, R. J. *J. Am. Chem. Soc.* **1992**, *114*, 160. (m) Rottink, M. K.; Angelici, R. J. *J. Am. Chem. Soc.* **1992**, *114*, 8296. (n) Sowa, J. R., Jr.; Bonanno, J. B.; Zanotti, V.; Angelici, R. J. *Inorg. Chem.* **1992**, *31*, 1370. (o) Sowa, J. R., Jr.; Zanotti, V.; Angelici, R. J. *Inorg. Chem.* **1993**, *32*, 848. (p) Skagestad, V.; Tilset, M. *J. Am. Chem. Soc.* **1993**, *115*, 5077.

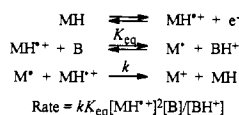
(3) (a) Tilset, M.; Parker, V. D. *J. Am. Chem. Soc.* **1989**, *111*, 6711; **1990**, *112*, 2843. (b) Parker, V. D.; Handoo, K. L.; Roness, F.; Tilset, M. *J. Am. Chem. Soc.* **1991**, *113*, 7493.

(4) (a) Edidin, R. T.; Sullivan, J. M.; Norton, J. R. *J. Am. Chem. Soc.* **1987**, *109*, 3945. (b) Protasiewicz, J. D.; Theopold, K. H. *J. Am. Chem. Soc.* **1993**, *115*, 5559.

(5) (a) Eisenberg, D. C.; Norton, J. R. *Isr. J. Chem.* **1991**, *31*, 55, and references cited. (b) Eisenberg, D. C.; Lawrie, C. J. C.; Moody, A. E.; Norton, J. R. *J. Am. Chem. Soc.* **1991**, *113*, 4888.

(6) (a) Ryan, O. B.; Tilset, M.; Parker, V. D. *J. Am. Chem. Soc.* **1990**, *112*, 2618. (b) Ryan, O. B.; Tilset, M.; Parker, V. D. *Organometallics* **1991**, *10*, 298. (c) Ryan, O. B.; Tilset, M. *J. Am. Chem. Soc.* **1991**, *113*, 9554. (d) Ryan, O. B.; Smith, K.-T.; Tilset, M. *J. Organomet. Chem.* **1991**, *421*, 315. (e) Tilset, M. *J. Am. Chem. Soc.* **1992**, *114*, 2740. (f) Zlota, A.; Tilset, M.; Caulton, K. G. *Inorg. Chem.*, in press. (g) Klingler, R. J.; Huffman, J. C.; Kochl, J. K. *J. Am. Chem. Soc.* **1980**, *102*, 208. (h) Detty, M. R.; Jones, W. D. *J. Am. Chem. Soc.* **1987**, *109*, 5666. (i) Chen, L.; Davies, J. A. *Inorg. Chim. Acta* **1990**, *175*, 41. (j) Westerberg, D. E.; Rhodes, L. F.; Edwin, J.; Geiger, W. E.; Caulton, K. G. *Inorg. Chem.* **1991**, *30*, 1107.

Scheme I



concentrations leading to less reversible voltammograms. This is consistent with a second-order reaction involving proton transfer from $\text{CpRu}(\text{PPh}_3)_2\text{H}^{+\bullet}$ to $\text{CpRu}(\text{PPh}_3)_2\text{H}$. We inferred that hydrides of the type $\text{CpRu}(\text{PR}_3)_2\text{H}$ could be suitable substrates for a detailed investigation of proton-transfer reactions from metal hydride cation radicals. When compared with carbonylmetal hydrides previously investigated by us,^{6a-c} the thermodynamic and kinetic acidities of these cation radicals are considerably attenuated, presumably by the electronic and steric effects exerted by the bulky phosphine donor ligands.

While the deprotonation reactions of *organic* cation radicals have been extensively studied and have revealed a fascinating complexity in terms of reaction mechanisms,⁷ thus far, quantitative investigations of the kinetics and mechanisms of the analogous reactions for metal hydrides remain scarce.⁸ Of particular relevance to the study presented here, it has been concluded that oxidation of $\text{ReClH}(\text{NCR})(\text{dppe})_2^+\text{BF}_4^-$ produced the dication radical $\text{ReClH}(\text{NCR})(\text{dppe})_2^{2+\bullet}$ which underwent deprotonation, most likely by a mechanism involving reversible transfer of H^+ from $\text{ReClH}(\text{NCR})(\text{dppe})_2^{2+\bullet}$ to the medium (solvent/electrolyte).^{8a,9} The reaction was terminated by rate-limiting homogeneous chemical oxidation of $\text{ReCl}(\text{NCR})(\text{dppe})_2^+$ by $\text{ReClH}(\text{NCR})(\text{dppe})_2^{2+\bullet}$. The mechanism is depicted in Scheme I, where MH represents $\text{ReClH}(\text{NCR})(\text{dppe})_2^+$ and B is the basic medium. In accord with the proposed mechanism, a second-order reaction with respect to the substrate concentration was established and an increase in the medium basicity was accompanied by a rate increase.

Herein, we provide details of an electrochemical investigation of the oxidation chemistry of the hydrides $\text{CpRu}(\text{PPh}_3)_2\text{H}$ (1), $\text{CpRu}(\text{dppm})\text{H}$ (2), $\text{CpRu}(\text{dppe})\text{H}$ (3), and $\text{CpRu}(\text{dppp})\text{H}$ (4).⁹ Especially, the mechanisms of the oxidatively-induced deprotonation reactions of 1 and 4 have been carefully studied. Kinetic parameters are reported for the apparent proton transfer from $1^{+\bullet}$ and $4^{+\bullet}$ to their 18-electron parent hydrides, and possible mechanisms for the proton-transfer reactions are discussed.

Results

Electrochemical One-Electron Oxidation of the Metal Hydrides.

We recently reported that cyclic voltammetry (CV) measurements showed that $\text{CpRu}(\text{PPh}_3)_2\text{H}$ (1) undergoes a chemically nearly reversible¹⁰ one-electron oxidation at -0.34 V vs the ferrocene/ferrocenium (Fc) couple in dichloromethane/0.2 M $\text{Bu}_4\text{N}^+\text{PF}_6^-$ at a Pt disk electrode.^{6d} Morris and co-workers have briefly described the oxidation chemistry of 1–4 and related Ru hydrides^{2b-4} and reported that the primary oxidation processes in all cases were chemically irreversible in dichloromethane and THF at the relatively slow voltage sweep rate $\nu = 0.25$ V/s. In

(7) (a) Parker, V. D. *Acc. Chem. Res.* **1984**, *17*, 243. (b) Hammerich, O.; Parker, V. D. *Adv. Phys. Org. Chem.* **1984**, *20*, 55. (c) Reitstøen, B.; Norrsell, F.; Parker, V. D. *J. Am. Chem. Soc.* **1989**, *111*, 8463. (d) Dinnocenzo, J. P.; Banach, T. E. *J. Am. Chem. Soc.* **1989**, *111*, 8646. (e) Parker, V. D.; Chao, Y.; Reitstøen, B. *J. Am. Chem. Soc.* **1991**, *113*, 2336. (f) Parker, V. D.; Tilsted, M. *J. Am. Chem. Soc.* **1991**, *113*, 8778.

(8) (a) Amatore, C.; Fraústo Da Silva, J. J. R.; Guedes Da Silva, M. F. C.; Pombelro, A. J. L.; Verpeaux, J.-N. *J. Chem. Soc., Chem. Commun.* **1992**, 1289. (b) Lemos, M. A. N. D. A.; Pombelro, A. J. L. *J. Organomet. Chem.* **1992**, *438*, 159.

(9) $\text{dppm} = \text{Ph}_2\text{PCH}_2\text{PPh}_2$; $\text{dppe} = \text{Ph}_2\text{PCH}_2\text{CH}_2\text{PPh}_2$; $\text{dppp} = \text{Ph}_2\text{PCH}_2\text{CH}_2\text{CH}_2\text{PPh}_2$.

(10) The term chemical reversibility refers to the stability of the electrode-generated cation radicals on the time scale of the CV experiments. For a chemically irreversible process, no peak is observed during the cathodic (return) scan; partial chemical reversibility results in an observable peak but with a ratio of cathodic to anodic peak currents of less than unity.

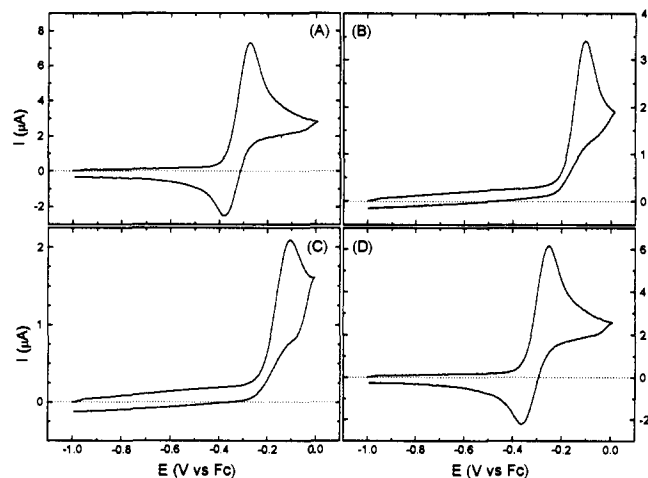


Figure 1. Cyclic voltammograms of (A) $\text{CpRu}(\text{PPh}_3)_2\text{H}$ (1); (B) $\text{CpRu}(\text{dppm})\text{H}$ (2); (C) $\text{CpRu}(\text{dppe})\text{H}$ (3); and (D) $\text{CpRu}(\text{dppp})\text{H}$ (4). Conditions: acetonitrile/THF (4:1), 0.1 M $\text{Bu}_4\text{N}^+\text{PF}_6^-$, $T = 0^\circ\text{C}$, $\nu = 1.0$ V/s, Au disk electrode ($d = 0.8$ mm for 1 and 4; 0.6 mm for 2 and 3). In this and subsequent plots, the anodic current is plotted as a positive current.

our hands, complexes 1, 3, and 4 give rise to partially reversible behavior in both solvents at this sweep rate, whereas the oxidation of 2 is irreversible. In acetonitrile, the oxidations of 1 and 4 are partially reversible, while 2 and 3 exhibit irreversible behavior at sweep rates of up to 100 V/s. The irreversibility that was seen for 1–4 by Morris most likely was caused by the fact that the CV switching potentials in these experiments were located beyond the occurrence of secondary, and irreversible, anodic processes.¹¹ This serves to deplete the diffusion layer of the cation radicals and results in an apparent decrease in the extent of chemical reversibility for the first electrode process. This conclusion has been supported by CV measurements in our laboratories.

We recently described^{6f} a voltammetric investigation of the oxidation chemistry of $\text{Cp}^*\text{Ru}(\text{PPh}_3)(\text{H})_3$ at Pt and Au disk electrodes. Molecular hydrogen which was generated as a consequence of the one-electron oxidation adsorbed at the Pt, but not at the Au, electrodes and interfered with the voltammetric response. Initial experiments in which 1 and 4 were oxidized at the Pt electrode revealed similar but less pronounced effects, and for this reason, Au electrodes have been consistently used in this work.

Figure 1 displays cyclic voltammograms for the oxidation of complexes 1–4 in 4:1 acetonitrile/THF at the Au disk electrode (the THF was added as a cosolvent to improve substrate solubility) containing 0.1 M $\text{Bu}_4\text{N}^+\text{PF}_6^-$ as the supporting electrolyte. It is seen that the oxidations of 1 and 4 are chemically almost reversible under these conditions (0°C , $\nu = 1.0$ V/s, substrate concentration 1.0 mM). Oxidation potentials were accurately determined by derivative cyclic voltammetry (DCV)¹² and are included in Table I. Peak potentials are reported for irreversible processes. For partially reversible processes, Table I lists the reversible potentials, taken as the midpoint between the anodic and cathodic peaks. Data from measurements in THF/0.2 M $\text{Bu}_4\text{N}^+\text{PF}_6^-$ are also included and are in good agreement with those previously reported.^{2b}

Interestingly, the extent of chemical reversibility for the oxidations of 1 and 4 was highly solvent dependent. This is illustrated in Figure 2, which shows CV traces for the oxidation of 4 in acetonitrile and THF. The ratio of the cathodic to anodic peak current is unity in THF but considerably less than unity in

(11) Morris, R. H. Personal communication.

(12) (a) Ahlberg, E.; Parker, V. D. *J. Electroanal. Chem., Interfacial Electrochem.* **1981**, *121*, 73. (b) Parker, V. D. *Acta Chem. Scand., Ser. B* **1984**, *B38*, 165. (c) Parker, V. D. In *Electroanalytical Chemistry*; Bard, A. J., Ed.; Marcel Dekker: New York, 1986; Vol. 14, p 1.

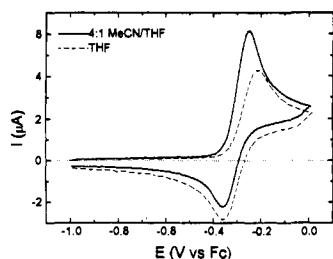


Figure 2. Cyclic voltammograms of CpRu(dppp)H (4) in acetonitrile/THF (4:1), 0.1 M Bu₄N⁺PF₆⁻ and in THF, 0.2 M Bu₄N⁺PF₆⁻. *T* = 0 °C, *v* = 1.0 V/s, Au disk electrode (*d* = 0.8 mm).

Table I. Electrochemical Data for the Oxidation of Hydrides 1–4

compound MH	<i>E</i> _{ox} (MH) ^a		<i>n</i> _{ox} ^d acetonitrile
	acetonitrile/THF 4:1 ^b	THF ^c	
CpRu(PPh ₃) ₂ H (1)	-0.30 ^e	-0.28 ^e	1.0(0.1)
CpRu(dppm)H (2)	-0.11 ^f	-0.08 ^f	1.0(0.03)
CpRu(dppe)H (3)	-0.11 ^f	-0.16 ^e	0.9(0.1)
CpRu(dppp)H (4)	-0.29 ^e	-0.26 ^e	0.9(0.1)

^a Oxidation potential for the oxidation of MH, V vs Fc. Measured by DCV¹¹ (*v* = 1.0 V/s, 0 °C, *d* = 0.8-mm Au disk electrode) on solutions containing 1.0 mM of substrate. ^b 0.1 M Bu₄N⁺PF₆⁻. ^c 0.2 M Bu₄N⁺PF₆⁻. ^d Faraday/mol transferred, from coulometry experiments. ^e Reversible potential, taken as the midpoint between the anodic and cathodic peaks. ^f Peak potential for irreversible wave.

acetonitrile. The follow-up reaction of 4^{•+} clearly proceeds faster in the more polar solvent. A cyclic voltammogram that was recorded in dichloromethane/0.2 M Bu₄N⁺PF₆⁻ at 0 °C within less than 30 s of dissolving the substrate also showed a fully reversible voltammogram. The substrate decomposed in this solvent within a few minutes, and this precluded the use of dichloromethane solvent for more detailed work.

Constant-current coulometry with DCV monitoring of the disappearance of the substrates indicated the consumption of 1 faraday/mol for the oxidation reactions (Table I), as expected for overall proton transfer from the cation radicals to the neutral hydrides in accordance with eq 2. When 10 equiv of pyrrolidine was added to the solutions before the coulometry experiments, the measurements showed the consumption of 2 faraday/mol, in agreement with the overall process shown in eq 1.

Chemical Oxidation of the Metal Hydrides. The occurrence of one-electron transfer reactions and subsequent proton transfer was supported by the observation (¹H NMR) of near 1:1 mixtures of the solvent-coordinated complexes CpRu(PR₃)₂(NCCD₃)⁺ and the dihydrides CpRu(PR₃)₂(H)₂⁺ (for 1, 3, and 4) and/or dihydrogen complexes CpRu(PR₃)₂(H)₂⁺ (for 2 and 3) when the hydrides were treated with 1 equiv of Cp₂Fe⁺PF₆⁻ in acetonitrile-d₃.

DCV Investigation of the Kinetics of the Reactions of 1^{•+} and 4^{•+} in 4:1 Acetonitrile/THF. The reactions of 1^{•+} and 4^{•+} in 4:1 acetonitrile/THF proceeded at rates that allowed for a mechanistic and kinetic analysis. Figure 3 shows a DCV^{12,13} trace for the oxidation of 4, obtained under conditions identical to those used for the normal voltammogram in Figure 1D. The cyclic voltammetry peak potentials are found at the points where the rapidly descending or ascending DCV curve crosses the base line after the derivative peaks labeled (a') and (b'), respectively. The cathodic (b') to anodic (a') derivative peak current ratio *R*'_i is

(13) For some examples of applications of DCV kinetics in organometallic chemistry, see: (a) Tilset, M.; Bodner, G. S.; Senn, D. R.; Gladysz, J. A.; Parker, V. D. *J. Am. Chem. Soc.* **1987**, *109*, 7551. (b) Aase, T.; Tilset, M.; Parker, V. D. *J. Am. Chem. Soc.* **1990**, *112*, 4974. (c) Tilset, M. In *Energetics of Organometallic Species*; Simões, J. A. M., Ed.; Kluwer Academic: Dordrecht, The Netherlands, 1992; p 109. (d) Tilset, M.; Skagestad, V.; Parker, V. D. In *Molecular Electrochemistry of Inorganic, Bioinorganic and Organometallic Compounds*; Pombeiro, A. J. L., McCleverty, J. A., Eds.; Kluwer Academic: Dordrecht, The Netherlands, 1993; p 269. (e) Pedersen, A.; Tilset, M. *Organometallics* **1993**, *12*, 56.

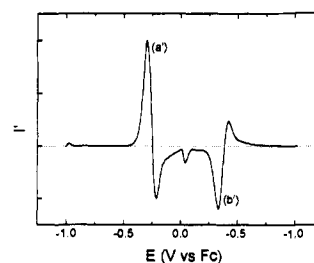


Figure 3. Derivative cyclic voltammogram for the oxidation of 4. Conditions are the same as given in the caption to Figure 1D.

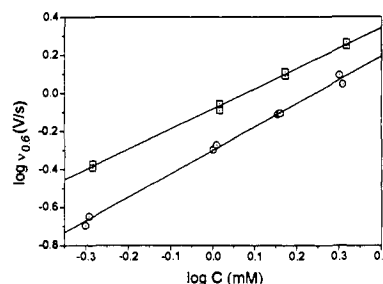


Figure 4. DCV reaction-order plot for the reactions of 1^{•+} (circles) and 4^{•+} (squares). Conditions: 0.1 M Bu₄N⁺PF₆⁻, 4:1 acetonitrile/THF, *d* = 0.8-mm Au disk electrode, *E*_{switch} - *E*_{rev} = 200 mV. *T* = 20 °C for 1^{•+} and 0 °C for 4^{•+}.

readily measured in DCV experiments. The DCV technique has the advantage that double-layer charging currents are eliminated and that the base line is well-defined for the forward and reverse scans.

The parameter *v*_{*c*} is defined as the voltage sweep rate which for defined experimental conditions causes *R*'_{*i*} to equal *c*. For example, *v*_{0.5} is obtained for *c* = 0.5, and the time lag between peaks (a') and (b') at this particular sweep rate correlates with the half-life of the electrode-generated intermediate. The rate constant for the follow-up chemical reaction is proportional to *v*_{*c*}. When the separation between the switching potential (*E*_{switch}) and the reversible electrode potential for the substrate oxidation (*E*_{rev}) is fixed in a series of experiments, DCV may be used in a reaction-order analysis to establish the rate law for the follow-up reaction.^{12c,14a} Activation energies *E*_a are available from simple Arrhenius-type correlations of ln(*v*_{*c*}/*T*) vs 1/*T*.^{12c,15} The actual rate constants are determined by comparison of experimental DCV data with theoretical data obtained by digital simulation when the overall rate law and the reaction stoichiometry are known.^{12c}

Figure 4 summarizes DCV reaction-order data for the oxidation of 1 and 4 in 4:1 acetonitrile/THF, 0.1 M Bu₄N⁺PF₆⁻ for substrate concentrations in the range of 0.5–2.0 mM. The plots of log *v*_{0.6} vs log[substrate] have slopes of 1.23(0.03) and 1.06(0.03), respectively (one standard error from the linear regression in parentheses). Ideally, a slope of 1.0 is expected for a process that is second order overall with respect to cation radical, substrate, and other possible electroactive species arising from the substrate. The absence of an upward curvature in the plot for 1 suggests that the somewhat greater than ideal slope is not due to the presence of higher-order processes. We conclude that the rate law for the reactions of the cation radicals is overall second order

(14) (a) A similar approach, based on normal cyclic voltammogram data, has been recently employed in an elegant study of key steps in the Heck reaction.^{14b} (b) Amatore, C.; Azzabi, M.; Jutand, A. *J. Am. Chem. Soc.* **1991**, *113*, 8375.

(15) Note that it is ln(*v*_{*c*}/*T*) vs 1/*T* and not ln(*v*_{*c*}) vs 1/*T* that results in an Arrhenius-type relationship.^{12c} This treatment yields *E*_a without prior knowledge about the reaction mechanism. In contrast, the preexponential frequency factor *A* is not available by this treatment unless *v*_{*c*} values are converted to rate constants—which *does* require knowledge about the mechanism.

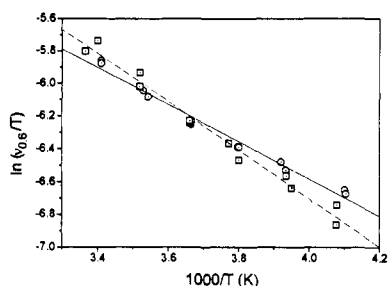


Figure 5. Arrhenius-type plot of $\ln(\nu_{0.6}/T)$ vs $1000/T$ for the reactions of 1^{*+} (circles, full line) and 4^{*+} (squares, dashed line). Conditions: 0.1 M $\text{Bu}_4\text{N}^+\text{PF}_6^-$, 4:1 acetonitrile/THF, $d = 0.8$ -mm Au disk electrode, $E_{\text{switch}} - E_{\text{rev}} = 200$ mV, 1.0 mM substrate.

in terms of neutral substrate, cation radical, and possible intermediates that derive from these and may enter into the rate law.

Figure 5 shows Arrhenius-type plots of $\ln(\nu_{0.6}/T)$ vs $1/T$ data¹⁵ from the DCV measurements of the same reactions, performed at 1.0 mM substrate concentrations. Linear regression yielded the activation energies E_a , determined to be 9.4(0.4) kJ/mol for the reaction of 1^{*+} and 12.3(0.6) kJ/mol for that of 4^{*+} (one standard error from the linear regression analysis in parentheses).

The $k_{\text{H}}/k_{\text{D}}$ ($= \nu_{0.6}(\text{H})/\nu_{0.6}(\text{D})$) kinetic isotope effects for the reactions of the metal hydrides **1** and **4** vs the deuterides **1-d** and **4-d** were measured. DCV analyses were performed on the hydrides and deuterides at 1.0 mM substrate concentrations at 0 °C. Measurements were performed a minimum of five times each on at least four independently-prepared solutions of each substrate and yielded $k_{\text{H}}/k_{\text{D}} = 0.94(0.06)$ for **1** vs **1-d** and $k_{\text{H}}/k_{\text{D}} = 0.90(0.10)$ for **4** vs **4-d**. There was some concern that the deuterium (D) label could undergo exchange via a protonation/deprotonation sequence involving protic impurities (water, etc.) in the electrolyte. As a control, kinetic measurements on **4-d** were performed in the presence of 1% (v/v) D_2O . The DCV $\nu_{0.6}$ data were unaffected by the presence of D_2O . As an extra check, it was verified that for **4**, the data were unaffected by the presence of 1% H_2O . Finally, **1-d** and **4-d** were recovered from the electrolyte solution after 1 h (more than twice the duration of the typical electrochemical experiments) and subjected to analysis by ^1H NMR spectroscopy. No evidence was found for loss of the D label in **1-d**; some (<30%) H/D exchange had occurred for **4-d**.

We conclude that the $k_{\text{H}}/k_{\text{D}}$ isotope effects are not significantly different from unity. This result is quite unexpected for a process that was initially considered to involve direct proton transfer from metal hydride cation radicals to the neutral hydrides.

Solvent Effect on the Rate of Reaction. The voltammograms in Figure 2 demonstrate a significantly enhanced reactivity of 4^{*+} in acetonitrile relative to THF. The dependence of the rate on the solvent composition was investigated for various THF/acetonitrile mixtures. In THF/0.1 M $\text{Bu}_4\text{N}^+\text{PF}_6^-$, $R'_i = 0.980$ was measured at 0.1 V/s (0.8-mm Au electrode, 0 °C, $E_{\text{switch}} - E_{\text{rev}} = 200$ mV). Digital simulation data^{16a} show that $\nu_{0.6}$ should be on the order of 1/40th of the $\nu_{0.98}$ value, or about 0.0025 V/s.^{16b} Table II shows DCV kinetic data for the reaction of 4^{*+} in THF/acetonitrile mixtures. There is a dramatic effect to be seen even with minute amounts of acetonitrile present. With as little as 1% acetonitrile by volume (but of course a huge molar excess relative to the substrate concentration), $\nu_{0.6}$ has increased 20-fold to 0.057 V/s! Increasing the amount of acetonitrile leads to an increasingly faster reaction, although the initial dramatic effect soon levels off. This is shown in the plot of $\nu_{0.6}$ vs acetonitrile

Table II. Dependence of $\nu_{0.6}$ on the Acetonitrile Concentration for the Reaction of 4^{*+} in Acetonitrile/THF Mixtures^a

[MeCN], % vol	$\nu_{0.6}$, V/s	[MeCN], % vol	$\nu_{0.6}$, V/s
0.0	0.0025 ^b	20.0	0.351
1.0	0.057	40.1	0.400
4.8	0.163	60.0	0.497
9.9	0.206	80.0	0.589
15.3	0.319	100.0	0.659

^a 0.1 M $\text{Bu}_4\text{N}^+\text{PF}_6^-$. ^b $R'_i = 0.980$ was measured at 0.1 V/s (0.8 mm Au electrode), 0 °C, $E_{\text{switch}} - E_{\text{rev}} = 200$ mV. $\nu_{0.6}$ was estimated from simulation data (see text).

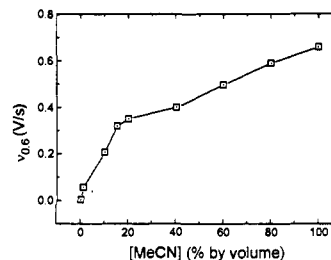


Figure 6. Dependence of $\nu_{0.6}$ (which is proportional to k_{obs}) for the reaction of 4^{*+} on the acetonitrile concentration.

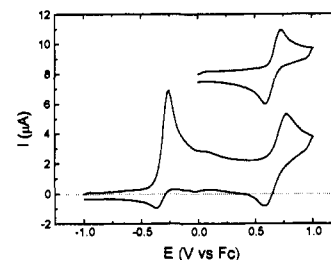


Figure 7. Cyclic voltammogram for the oxidation of $\text{CpRu}(\text{dppp})\text{H}$ (major trace) and $\text{CpRu}(\text{dppp})(\text{NCMe})^+\text{PF}_6^-$ (insert, top right). Conditions are the same as in the caption to Figure 1D.

concentration in Figure 6. The effect at low [MeCN] appears too dramatic to be attributable to a bulk solvent effect and most likely suggests that acetonitrile is directly involved in the reaction of 4^{*+} on a molecular level, i.e., as a stoichiometric participant. It is clear that the effect is not due to the basicity of acetonitrile, since as mentioned already, the presence of 1% by volume of H_2O had no effect on the rate of the reaction. The proton-accepting ability of H_2O greatly exceeds that of acetonitrile even at low H_2O concentrations.¹⁷

Oxidation of the Metal Hydride Cation Radicals to Dications.

Jia and Morris reported that cyclic voltammograms of compounds **1–4** showed a second, irreversible oxidation wave ca. 0.5–0.8 V anodic of the wave arising from oxidation to the monocation.²⁸ The more anodic processes were tentatively attributed to oxidation to the dications. In a different work, Detty and Jones^{6b} observed that oxidation of $\text{CpRe}(\text{PPh}_3)_2\text{H}_2$ and analogues yielded stable cation radicals. An electrocatalytic chain reaction was initiated by further oxidation to the dication, resulting in the formal H^+ -transfer products $\text{CpRe}(\text{PPh}_3)_2(\text{NCMe})\text{H}^+$ and $\text{CpRe}(\text{PPh}_3)_2\text{H}_3^+$. These reports alerted us that dications might be involved in the chemical reactions of 1^{*+} and 4^{*+} and called for a careful analysis of this possibility.

Figure 7 shows a cyclic voltammogram for the oxidation of **4** in 4:1 acetonitrile/THF at $\nu = 1.0$ V/s. At potentials anodic of the $4/4^{*+}$ wave, a faint, apparently reversible wave is seen at ca. 0.1 V vs Fc. Except for the reversibility, this wave has the appearance of the wave attributed to the chain-initiating oxidation of $\text{CpRe}(\text{PPh}_3)_2\text{H}_2^{*+}$ to the dication in the work of Detty and Jones. In addition, a chemically reversible wave is centered at 0.70 V. This wave coincides with the reversible oxidation wave

(16) (a) Based on a disproportionation mechanism; vide infra. (b) The simulated value for R'_i in the case of no follow-up reaction is 1.034. The profile of R'_i vs ν is rather flat when R'_i is near unity, and therefore, significant uncertainty is involved when $\nu_{0.6}$ values are extrapolated from $\nu_{0.98}$ measurement data.

(17) Coetzee, J. F. *Progr. Phys. Org. Chem.* 1967, 4, 45.

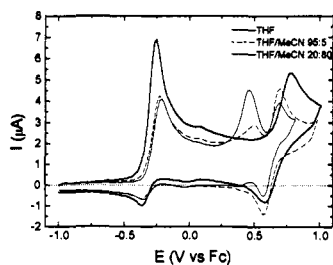


Figure 8. Cyclic voltammograms for the oxidation of CpRu(dppp)H in THF/acetonitrile mixtures; $d = 0.8$ -mm Au disk electrode, $\nu = 1.0$ V/s, $T = 0$ °C.

of CpRu(dppp)(NCMe)⁺ (insert in Figure 7). It is reasonable from the kinetic investigation presented earlier that significant amounts of this product form on the time scale of the 1 V/s scan depicted in Figure 7. However, it was more surprising to see that at 20 V/s, this wave was still present with the same intensity (relative to that of the 4/4⁺ wave), since on this time scale, 4⁺ should essentially undergo no reaction. Furthermore, at 20 V/s, the wave appeared to be chemically only partially reversible. These observations may indicate that by coincidence, the wave is due to overlapping signals due to the chemically irreversible oxidation of 4⁺ to 4²⁺ (predominant at high ν) and the chemically reversible oxidation of CpRu(dppp)(NCMe)⁺ (predominant at low ν). The other oxidation product, CpRu(dppp)(H)₂⁺, did not undergo oxidation at $E < 2.0$ V vs Fc.

On the basis of the work of Detty and Jones, we still found it necessary to check the possibility that the faint wave at 0.1 V vs Fc could be involved in a catalytic reaction which rapidly consumed 4⁺, thereby producing CpRu(dppp)(NCMe)⁺ even on the time scale of the 100 V/s measurements. In order to test this possibility, a series of DCV experiments were performed in which R'_i was measured for a wide range of scan reversal potentials at constant ν . If the wave was somehow involved in catalyzing the chemistry, then a rather abrupt change in R'_i vs E_{switch} should be observed as E_{switch} was moved from a position cathodic of the 0.1-V wave to a position anodic of it. However, a plot of R'_i vs $E_{\text{switch}} - E_{\text{ox}}(4)$ resulted in a smooth curve showing an exponential decay in R'_i for $E_{\text{switch}} - E_{\text{ox}} = 200$ –480 mV. An almost perfect match was seen between measured and simulated data for a disproportionation mechanism (vide infra), and there is no reason to suspect involvement of any undesired chain processes.

In THF/0.1 M Bu₄N⁺PF₆⁻, the second, irreversible oxidation wave was seen at 0.46 V vs Fc (Figure 8) and a third wave was located at 0.70 V. The wave at 0.46 V quickly dropped in intensity and moved toward the wave at 0.70 V when acetonitrile was gradually added to the electrolyte. This happened at the Au as well as at the Pt electrode. The reason for this behavior is unclear and leaves some uncertainty as to the correctness of the assignment of the secondary electrode processes.

The oxidation of 1 beyond the 1/1⁺ couple in acetonitrile/THF had some of the same characteristics as that of 4, although the waves were generally broader and less well-defined. Secondary waves were also seen for 2 and 3. However, for 2 and 3, the waves certainly cannot be due to oxidation of the cation radicals to the dications. On the time scale of the CV measurements, 2⁺ and 3⁺ have ample time to undergo essentially complete chemical reaction and therefore cannot be further oxidized to the dications. For these two compounds, the more anodic waves most likely arise exclusively from the oxidation of the products generated from the homogeneous reactions of 2⁺ and 3⁺.

X-ray Crystal Structure of 1. Although X-ray structures for a number of three-legged piano-stool derivatives of the type CpRu(PR₃)₂X have been determined,¹⁸ it appears that CpRu-

(dppp)H is the only hydride that has been structurally characterized thus far.¹⁹ The structure of 1 was determined, so that the steric properties of 1 and 4, the cations of which were kinetically most stable in the series described in this paper, could be assessed.

Selected bond lengths and angles are given in Table III. Figure 9 shows an ORTEP plot of the molecular structure of 1. The hydride ligand was located from a difference Fourier map; the Ru–H distance turned out to be 1.51(4) Å, which compares well with 1.55(5) Å determined for CpRu(dppp)H. Inspection of a computer-generated, space-filling model based on the X-ray structure shows that the hydride ligand, barely visible from the outside, is effectively shielded by the PPh₃ ligands against attack by bulky external reagents. Another interesting feature of the structure is the two nearly parallel phenyl-ring planes of C21–C26 and C61–C66. Four pairs of C–C separations are in the interval of 3.5–3.6 Å, and it is possible that an intramolecular stacking effect stabilizes the molecular structure.

Discussion

Bond Dissociation Energies of Cationic Dihydrides and Coordinated Dihydrogen Ligands. The reversible oxidation potentials of 1 and 4, along with the known pK_a values^{2a,20a} of the corresponding dihydrides CpRu(PPh₃)₂(H)₂⁺ ($pK_a = 15.8$ in acetonitrile), CpRu(dppe)(H)₂⁺ (15.3), and CpRu(dppp)(H)₂⁺ (16.4), may be combined by the use of a previously described thermochemical cycle^{3a,b} to arrive at the enthalpy-based bond dissociation energies (BDEs) for the cationic dihydrides.²¹ Thus, the Ru–H BDE for CpRu(PPh₃)₂(H)₂⁺ is calculated to be 310 kJ/mol and for CpRu(dppp)(H)₂⁺, 315 kJ/mol. If we assume that the reversible oxidation potential for 3 (vs Fc) is identical in THF and acetonitrile, then a BDE of 321 kJ/mol is calculated for CpRu(dppe)(H)₂⁺. Interestingly, assuming that the BDE of the phosphine-substituted complexes is not vastly different from that of CpRu(CO)₂H (272 kJ/mol^{3b}), the BDEs for the cationic dihydrides are consistently higher than the BDEs of the neutral monohydrides. The same situation was seen for CpW(CO)₂(PMe₃)(H)₂⁺ (>318 kJ/mol^{6a}) vs CpW(CO)₂(PMe₃)H (293 kJ/mol^{3b}). It should be noted that the BDE data for the dihydrides represent the BDEs for cleavage of the *first* hydride ligand from these complexes, rather than average BDEs for the two hydride ligands.

In solution, CpRu(dppe)(H)₂⁺ exists in equilibrium with the dihydrogen complex²² CpRu(dppe)(H₂)⁺, while the dpmm analogue exists only in the dihydrogen form CpRu(dpmm)(H₂)⁺.²⁸ The electrode potentials for the oxidation of 2 and 3 again may be combined with pK_a data to yield the pertinent BDE values. In this case, the data should be considered to represent the *BDEs of the coordinated H₂ ligand in the dihydrogen complexes*.²⁸ Thus, the BDE(H–H) of CpRu(dppe)(H₂)⁺ is calculated to be 319 kJ/mol, based on the reversible electrode potential in THF and a pK_a of 15.0. The BDE of CpRu(dpmm)(H₂)⁺ is 328 kJ/mol, based on the irreversible potential, which may be in error due to an unknown kinetic potential shift which has not been corrected for, and a pK_a of 15.3. Considering that the value for

(19) Litster, S. A.; Redhouse, A. D.; Simpson, S. J. *Acta Crystallogr., Sect. C* **1992**, *C48*, 1661.

(20) (a) The reported pK_a values, referred to an aqueous scale, have been converted to an acetonitrile scale by adding 7.8 pK_a units as described elsewhere,^{20b} reflecting the difference in solvation energy for the proton in water and acetonitrile of 11 kcal/mol.^{20c} (b) Jia, G.; Morris, R. H. *Inorg. Chem.* **1990**, *29*, 581. (c) Kolthoff, I. M.; Chantooni, M. K., Jr. *J. Phys. Chem.* **1972**, *76*, 2024.

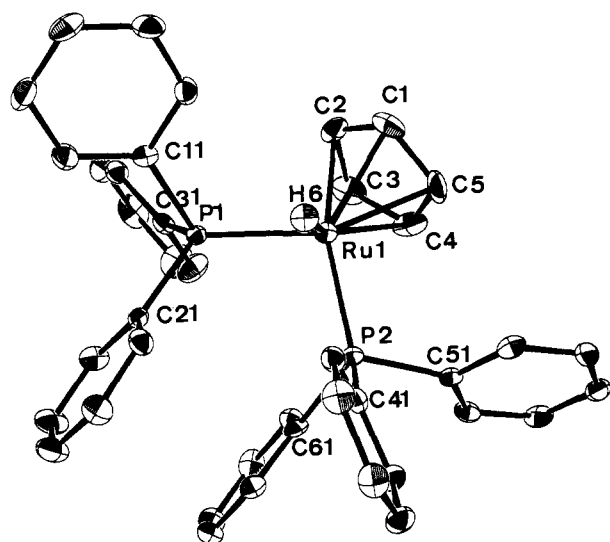
(21) BDE(MH) = 5.704 pK_a + 96.485 $E^\circ_{\text{ox}}(\text{M}^+) + 249$ kJ/mol when measurements are performed in acetonitrile and oxidation potentials are reported vs Fc at 25 °C.

(22) For reviews of the chemistry of dihydrogen complexes, see: (a) Kubas, G. J. *Acc. Chem. Res.* **1988**, *21*, 120. (b) Crabtree, R. H.; Hamilton, D. G. *Adv. Organomet. Chem.* **1988**, *28*, 299. (c) Crabtree, R. H. *Acc. Chem. Res.* **1990**, *23*, 95. (d) Jessop, P. G.; Morris, R. H. *Coord. Chem. Rev.* **1992**, *121*, 155.

(18) For a recent review of the chemistry of the CpRu(PR₃)₂ auxiliary, see: Davies, S. G.; McNally, J. P.; Smallridge, A. J. *Adv. Organomet. Chem.* **1990**, *30*, 1.

Table III. Selected Bond Lengths (Å) and Angles (deg)^a

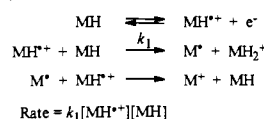
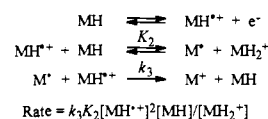
			Bond Lengths				
RU1-H6	1.51(4)	RU1-Cp(cent)	1.889	P1-C21	1.843(3)	P1-C31	1.848(3)
RU1-P1	2.256(1)	RU1-P2	2.265(1)	P2-C41	1.844(3)	P2-C51	1.858(3)
RU1-C1	2.233(3)	RU1-C2	2.235(3)	P2-C61	1.852(3)	C1-C2	1.395(5)
RU1-C3	2.260(4)	RU1-C4	2.232(4)	C1-C5	1.419(5)	C2-C3	1.424(5)
RU1-C5	2.226(3)	P1-C11	1.857(3)	C3-C4	1.407(5)	C4-C5	1.401(6)
			Bond Angles				
P1-RU1-P2	101.4(1)	P1-RU1-Cp(cent)	124.8	RU1-P2-C41	123.6(1)	RU1-P2-C51	109.8(1)
P1-RU1-H6	73.2(15)	P2-RU1-Cp(cent)	125.4	RU1-P2-C61	117.9(1)	C41-P2-C51	97.3(2)
P2-RU1-H6	92.7(15)	H6-RU1-Cp(cent)	125.0	C41-P2-C61	101.2(2)	C51-P2-C61	103.7(2)
RU1-P1-C11	115.6(1)	RU1-P1-C21	122.1(1)	C1-C2-C3	108.9(3)	C2-C1-C5	107.6(3)
RU1-P1-C31	113.0(1)	C11-P1-C21	98.8(2)	C2-C3-C4	106.6(3)	C3-C4-C5	109.0(3)
C11-P1-C31	102.6(2)	C21-P1-C31	102.0(2)	C1-C5-C4	107.8(3)		

^a The centroid of the Cp ring is denoted by Cp(cent).**Figure 9.** ORTEP drawing of the molecular structure of **1** with hydrogen atoms (except hydride) removed for clarity.

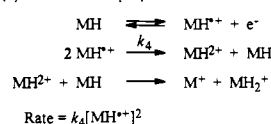
the BDE(H-H) in molecular H₂ is 436 kJ/mol,²³ the coordination of H₂ at the cationic Ru centers activates the H₂ molecule toward homolysis by more than 100 kJ/mol. This bond weakening, of course, is qualitatively in accord with the reductions in ν_{H-H} stretching frequencies and force constants that are found when the H₂ molecule is coordinated and with the theories of bonding in dihydrogen complexes.²²

Thermochemical Aspects of the Deprotonation Reaction. The overall experimental results presented here, along with established knowledge about the reactions of metal hydride cation radicals, leave little doubt that proton transfer is the net reaction of the cations. The cyclic voltammetry and coulometry measurements in the presence and absence of added base as well as the outcome of the homogeneous oxidations with ferrocene are consistent with this conclusion. We will now look at available pK_a and related data to show that such a process is indeed viable from a thermochemical point of view.

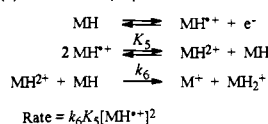
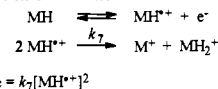
The pK_a of CpRu(CO)₂H has been determined to be 20.2 in acetonitrile.^{2d} The substitution of PPh₃ and other phosphine ligands for CO is known to greatly affect the pK_a values of related hydrides: pK_a = 14.2 for Mn(CO)₅H^{2a} vs 20.4 for Mn(CO)₄(PPh₃)H;^{2e} 8.3 for Co(CO)₄H vs 15.4 for Co(CO)₃(PPh₃)H;^{2d} and 13.3 for CpCr(CO)₃H^{2c} vs 21.8 for CpCr(CO)₂(PPh₃)H.^{3b} The data for this limited number of complexes show that the lower the number of remaining COs left to accommodate the increased electron density caused by the substitution of PPh₃ for a CO, the greater is the corresponding hydride pK_a increase. A rough extrapolation suggests that a double PPh₃ substitution at

Scheme II(a) Irreversible H⁺ transfer(b) Reversible H⁺ transfer

(c) Irreversible disproportionation



(d) Reversible disproportionation

(e) Irreversible H⁺ transfer

CpRu(CO)₂H will bring the pK_a of CpRu(PPh₃)₂H up to about 40 in acetonitrile.

On the basis of previous work, metal hydride acidities increase by ca. 20–25 pK_a units as a consequence of a one-electron oxidation.^{2p,6a,b,e} The acidity of the cation radical 1^{+\bullet} will then be in the range of 15–20. Bases whose conjugate acids have pK_as in this range should therefore be capable of deprotonating the cation radical. Even somewhat unfavorable proton-transfer reactions can be driven by the subsequent irreversible oxidation of the radical CpRu(PPh₃)₂[•]. The acetonitrile pK_a of 15.8 for the dihydride complex CpRu(PPh₃)₂(H)₂⁺ suggests that a direct proton transfer from 1^{+\bullet} to **1** may be possible.

Discussion of Possible Mechanisms for the Proton-Transfer Reactions. The DCV analysis has established that the reactions of 1^{+\bullet} and 4^{+\bullet} follow second-order kinetics with respect to substrate, cation radical, and, if necessary, other intermediates arising from the substrate and that *k*_H/*k*_D isotope effects significantly different from unity are not observed. At first sight, a mechanism similar to that reported^{8a} for the deprotonation of ReClH(NCR)(dppe)₂²⁺ (Scheme I) could be envisioned. However, a reversible proton transfer to the *medium* can be discounted for the CpRu(PR₃)₂H^{+\bullet} complexes because of their relatively high pK_a values. Scheme II summarizes five alternative reaction mechanisms that will give rise to the observed second-order kinetics. In this scheme, MH₂⁺ and M⁺ signify the final products. (The reaction of 16-electron M⁺ with the solvent to yield MS⁺ is assumed to always be fast and will not affect the kinetics. Similarly, rapid solvent coordination at the 16-electron dication MH₂²⁺ will bear no effect on the observed rate law.) Mechanism a involves rate-limiting proton transfer from MH^{+\bullet} to MH followed by oxidation of the resulting radical M[•] and b shows a reversible proton transfer from MH^{+\bullet} to MH and a rate-determining oxidation of the radical M[•]. Mechanism c is an irreversible disproportionation of the cation radical followed by

(23) *CRC Handbook of Chemistry and Physics*; Lide, D. R., Ed.; CRC Press: Boca Raton, FL, 1992.

rapid proton transfer from the dication MH^{2+} to MH , while d represents a reversible disproportionation and rate-limiting proton transfer to MH . (Note that a reversible disproportionation followed by rate-limiting proton transfer from MH^{2+} to the medium will result in overall first-order kinetics with a rate proportional to $[\text{MH}^{2+}]^2/[\text{MH}]$. In this case, the stoichiometry would be unchanged, provided that the medium rapidly transferred the proton to the much more basic substrate.) Finally, e constitutes a H^+ -transfer reaction; this reaction will be kinetically indistinguishable from c and d.

Published simulation data for the DCV response for a number of electrode reaction mechanisms have established that a linear relationship exists between $\ln R'_i$ (R'_i is defined as the derivative peak current ratio for the reverse and forward voltammetric scans) and $\ln \nu$ when $0.3 < R'_i < 0.7$.^{12c} The slope of the plots of theoretical data for $\ln R'_i$ vs $\ln \nu$ depends on the particular electrode mechanism in question and can be used to distinguish between reactions that exhibit the same overall reaction order but differ in rate laws and/or reaction stoichiometries. For $E_{\text{switch}} - E_{\text{rev}} = 200$ mV, simulation data yield slopes of 0.363 for mechanism a,^{12c} 0.174 for b,²⁴ and 0.295 for c-e.^{12c}

The slopes for experimental $\ln R'_i$ vs $\ln \nu$ data were calculated and found to be 0.25(0.01) for 1 and 0.24(0.01) for 4. While these numbers do not accurately match the theoretical data for any of the above mechanisms, they certainly are in best agreement with mechanisms c-e. Calculated rate constants based on R'_i data obtained for $\nu = 0.4$ -1.6 V/s had a standard deviation of 7% for mechanisms c-e, 16% for a, and 26% for b. The lack of any observable $k_{\text{H}}/k_{\text{D}}$ isotope effect also renders mechanism a unlikely. Norton and co-workers have reported primary isotope effects of 3.6-3.7 for the self-exchange proton-transfer reactions between $\text{CpM}(\text{CO})_3\text{H}$ and $\text{CpM}(\text{CO})_3^-$ ($\text{M} = \text{Cr}, \text{Mo}, \text{and W}$).^{4a} More relevant data for nondegenerate proton-transfer reactions between metals unfortunately appear to not be available. The proton transfer in mechanism a may be thermodynamically downhill and therefore may possibly exhibit a smaller isotope effect than those observed in Norton's systems. However, preliminary results from our laboratories show that even more favorable H^+ transfers from 1^{2+} to added bases have $k_{\text{H}}/k_{\text{D}}$ isotope effects in the range of 2-3.²⁵ It is therefore not unreasonable to expect sizeable isotope effects for a reaction that follows mechanism a.

The reversible proton transfer depicted in b can also be discounted. The difference between measured and observed slopes of $\ln R'_i$ vs $\ln \nu$ is rather substantial. Furthermore, kinetic measurements for the reaction of 4^{2+} were performed in the presence of as much as 10 equiv of $\text{CpRu}(\text{dppp})(\text{H})_2^+\text{BF}_4^-$, but the reaction rate was insensitive to the presence of the latter. A significant rate retardation should be observed if rate law b was operative. It was checked and verified by ^1H NMR spectroscopy that $\text{CpRu}(\text{dppp})(\text{H})_2^+\text{BF}_4^-$ was stable in acetonitrile on the time scale involved in preparing the solution and performing the CV measurements.

In mechanism e, H^+ transfer occurs in the rate-limiting step. This event is expected to lead to a significant $k_{\text{H}}/k_{\text{D}}$ kinetic isotope effect. No $k_{\text{H}}/k_{\text{D}}$ data for H/D transfer between organometallic radicals are presently available. We note that Norton and co-workers found that $k_{\text{H}}/k_{\text{D}} = 2.8$ for the exothermic transfer of H^+/D^+ from $\text{Mn}(\text{CO})_5\text{H}/\text{Mn}(\text{CO})_5\text{D}$ to $(p\text{-}t\text{-BuC}_6\text{H}_4)_3\text{C}^+$.^{5a} While this reaction obviously is not a perfect model, we conclude that mechanism e is unlikely due to the lack of detectable kinetic isotope effects. Also, this mechanism is not readily reconciled with the dramatic effect on the kinetics in THF by addition of small amounts of acetonitrile.

By the method of elimination, the overall transfer of H^+

Table IV. Variable-Temperature Data for k vs T for the Reactions of 1^{2+} and 4^{2+} in 4:1 Acetonitrile/THF, 0.1 M $\text{Bu}_4\text{N}^+\text{PF}_6^-$ ^a

	substrate			
	CpRu(PPh ₃) ₂ H (1)		CpRu(dppp)H (4)	
	T (°C)	k (M ⁻¹ s ⁻¹)	T (°C)	k (M ⁻¹ s ⁻¹)
run 1	-29.3	1585	-28.0	1333
	-18.1	1882	-20.0	1669
	-9.8	2060	-10.0	1979
	-0.4	2412	0.0	2486
	10.2	2902	11.0	3095
run 2	20.1	3495	24.0	3849
	-29.5	1551	-28.0	1505
	-19.0	1787	-19.0	1798
	-10.0	2057	-8.0	2190
	-0.3	2366	0.0	2509
	9.1	2796	11.0	3369
	20.1	3436	21.0	4114

^a DCV $\nu_{0.6}$ data ($E_{\text{switch}} - E_{\text{rev}} = 200$ mV) have been converted to second-order rate constants as explained in the text.

probably occurs by one of the disproportionation mechanisms. The absence of a detectable kinetic isotope effect then dictates that mechanism c, rather than d, operates. Although no data are available for the acidities of the dications MH^{2+} , their $\text{p}K_{\text{a}}$ s must be sufficiently low that even the medium (and not only MH , as shown in Scheme II) is sufficiently basic to effect their deprotonation.²⁶

The measured $\nu_{0.6}$ values from the DCV kinetics can now be converted to second-order rate constants k by comparison with simulation data for the disproportionation mechanism.^{12c} Table IV lists calculated k vs T data representing two independent variable-temperature measurement series for each substrate in the temperature range of -29-21 °C. Eyring plots of k vs $1/T$ yield the following kinetic parameters for the reactions in 4:1 acetonitrile/THF: for 1^{2+} , $\Delta H^\ddagger = 7.2(0.4)$ kJ/mol, $\Delta S^\ddagger = -153(2)$ J/(K·mol), and $k(0^\circ\text{C}) = 2490$ M⁻¹ s⁻¹ by interpolation and for 4^{2+} , $\Delta H^\ddagger = 10.0(0.6)$ kJ/mol, $\Delta S^\ddagger = -142(2)$ J/(K·mol), and $k(0^\circ\text{C}) = 2581$ M⁻¹ s⁻¹. Uncertainties in parentheses are listed as one standard error resulting from the linear regression analysis based on combined data for the two runs.

Disproportionation Mechanism. The equilibrium constant for the disproportionation of 1^{2+} may be calculated to be at most 2.8×10^{-13} ($\Delta G^\circ_{273} > 66$ kJ/mol). These numbers are conservatively estimated from the $1/1^{2+}$ and $1^{2+}/1^{2+}$ redox potentials, based on $\Delta E = 0.68$ V seen in the voltammogram that was recorded when THF was the solvent (the acetonitrile data will result in an even more unfavorable equilibrium constant). The value represents an upper limit for the equilibrium constant due to the chemical irreversibility and, therefore, unknown kinetic potential shift of the second electrode process. This equilibrium constant is too low for a reversible disproportionation of two 1^{2+} species to be possible. Even if the reversible disproportionation is followed by a diffusion-controlled deprotonation by a species with a concentration of 0.1 M (i.e., supporting electrolyte anion) ($k_6 = \text{ca. } 10^{10}$ M⁻¹ s⁻¹), then the maximum attainable overall rate constant $k_{\text{obs}} = K_5 k_6$ will be ca. 10^{-4} M⁻¹ s⁻¹, which is about 7 orders of magnitude lower than the observed rate constants (vide infra). The direct irreversible disproportionation also seems impossible: ΔG^\ddagger for the electron transfer must be equal to or exceed the calculated ΔG° . From the kinetic parameters, at 0 °C, $\Delta G^\ddagger = 49$ kJ/mol which is much less than the minimum value of 66 kJ/mol for ΔG° for the disproportionation.

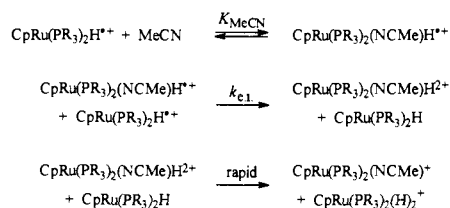
The dramatic effect that was seen for the reaction rate when minute amounts of acetonitrile were added to the THF medium instead suggests that 19-electron adducts of the type Cp-

(24) The mechanism was simulated as part of this work. Simulations were performed using Feldberg's method of finite differences; see: Feldberg, S. W. *Electroanal. Chem.* 1969, 3, 199.

(25) Smith, K.-T.; Tilset, M. Work in progress.

(26) This assumption is supported by the observation that the $\text{p}K_{\text{a}}$ differences between organic dications and cation radicals by far exceed the differences between cation radicals and neutrals of the same species; see: Parker, V. D.; Tilset, M. *J. Am. Chem. Soc.* 1988, 110, 1649.

Scheme III



$\text{Ru}(\text{PR}_3)_2(\text{NCMe})\text{H}^{*+}$ are involved in the disproportionation process. It is firmly established that the disproportionation of 17-electron organometallic radicals can be facilitated by the prior coordination of two-electron-donor molecules. Coordination of a donor at a 17-electron center generates a 19-electron intermediate with greatly enhanced reducing power.²⁷ We recently reported²⁸ that the difference between the oxidation potential for $\text{CpW}(\text{CO})_3\text{CH}_3$ ($E_p = 0.55$ V vs Fc) and the reduction potential for $\text{CpW}(\text{CO})_3(\text{NCMe})\text{CH}_3^{2+}$ ($E_p = -0.80$ V vs Fc) amounted to at least 1.35 V—in other words, the reduction potential of 17-electron $\text{CpW}(\text{CO})_3\text{CH}_3^{*+}$ is shifted 1.35 V in the cathodic direction when acetonitrile coordinates to generate the 19-electron species $\text{CpW}(\text{CO})_3(\text{NCMe})\text{CH}_3^{*+}$.

The availability of 19-electron adducts of the type $\text{CpRu}(\text{PR}_3)_2(\text{L})\text{H}^{*+}$ is supported by the recent communication^{29a} that the 17-electron cation $\text{Cp}^*\text{Fe}(\text{dppe})\text{H}^{*+}$ (the deuteride analogue of which was characterized by X-ray crystallography^{29b}) gives a stable 19-electron CO adduct $\text{Cp}^*\text{Fe}(\text{CO})(\text{dppe})\text{H}^{*+}$. This adduct is presumably stabilized by the π -acceptor power of the CO ligand (note the low value for ν_{CO} of 1940 cm^{-1} for this cation). Acetonitrile adducts of 1^{*+} and 4^{*+} are not expected to be as stable due to electronic effects but at least should be considered to be available as intermediates in reactions. At sufficiently high concentrations of the 19-electron adducts, a further oxidation at the electrode might even be of importance. Still, an overall one-electron process would result due to the facile H^+ transfer from the 18-electron dication to the neutral parent. However, H^+ transfer to the medium would lead to first-order kinetics; rate-limiting H^+ transfer to the neutral parent would give second-order behavior requiring a kinetic isotope effect. Therefore, we conclude that the disproportionation and the subsequent proton transfer occur in the diffusion layer and not at the electrode.

The overall disproportionation/proton-transfer reaction, then, is best described as the three-step process in Scheme III. With reversible acetonitrile coordination and rate-limiting electron transfer, the observed ΔH^* is actually a composite quantity equal to the sum of ΔH° for the acetonitrile coordination and ΔH^* for the electron transfer. The latter can be expected to be low for the highly exothermic electron transfer; the former is unknown, but it has been reported that the formation of 19-electron adducts from 17-electron precursors is often thermodynamically downhill ($\Delta G^\circ < 0$).^{27a,30} The low measured values for ΔH^* therefore do not appear unreasonable. The highly negative entropies of activation, ca. $-150\text{ J}/(\text{K}\cdot\text{mol})$, also agree with this interpretation. In comparison, values for ΔS^* for the self-exchange reactions (in which there is no reason to suspect solvent coordination) of $\text{CpM}(\text{CO})_3\text{H}$ ($M = \text{Cr}, \text{Mo}, \text{and W}$) in acetonitrile were near $-100\text{ J}/(\text{K}\cdot\text{mol})$.^{4a}

Concluding Remarks. Somewhat surprisingly, experimental evidence suggests that the proton-transfer reactions of 1^{*+} and 4^{*+} to their neutral parents proceed by a disproportionation

mechanism rather than by a direct proton transfer, despite the fact that thermodynamic considerations indicate that a direct process should be feasible. We suspect that the sterically demanding phosphine ligands block the access to the protons in 1^{*+} and 4^{*+} for the bulky bases 1 and 4. As a result, the disproportionation mechanism provides a lower-energy pathway, at least when a good two-electron donor (but poor base!) like acetonitrile is present. It is still possible that the exceedingly slow reaction in the absence of acetonitrile is a direct proton-transfer process.

Contrasting the behavior of 1^{*+} and 4^{*+} , the reactions of 2^{*+} and 3^{*+} were significantly faster, although the thermodynamics should be comparable. The reactivity difference may be attributed to different steric effects. The smaller bite angles of dppe and dppe render the hydride sites of 2^{*+} and 3^{*+} more exposed toward attack by external reagents. It is presently not known whether these react by the same mechanisms as 1^{*+} and 4^{*+} or if a direct proton transfer operates here.

The results indicate that the reaction pathways open to metal hydride cation radicals are highly dependent on the combined steric and electronic effects of the substrate and the attacking base. Work in progress is aimed at delineating the reactivity patterns of these and related hydrides in the presence of sterically less hindered bases.

Experimental Section

General Procedures. All manipulations involving organometallic compounds were carried out with the use of vacuum-line, Schlenk, syringe, or drybox techniques. Acetonitrile was distilled from P_2O_5 , and acetonitrile- d_3 , dichloromethane, and dichloromethane- d_2 were distilled from CaH_2 . THF was distilled from sodium benzophenone ketyl. Dry methanol was distilled from magnesium metal. The electrochemical instrumentation, cells, data handling procedures, and electrodes have been previously detailed.^{12c,31} Acetonitrile/THF (4:1) containing $0.1\text{ M Bu}_4\text{N}^+\text{PF}_6^-$ was used as solvent for electrochemical experiments unless otherwise mentioned and was passed through a column of active neutral alumina before use to remove water and protic impurities. The electrolyte was freed of air by purging with purified argon, and all measurements and electrolyses were carried out under a blanket of solvent-saturated argon. ^1H NMR spectra were recorded on Varian-Gemini 200 or Varian XL-300 instruments. Chemical shifts are reported in parts per million relative to tetramethylsilane, with the residual solvent proton resonance as internal standards (δ 1.93 for acetonitrile- d_3 , 5.32 for dichloromethane- d_2 , and 7.15 for benzene- d_6).

The compounds $\text{CpRu}(\text{PPh}_3)_2\text{Cl}$, $\text{CpRu}(\text{PPh}_3)_2\text{H}$ (1), $\text{CpRu}(\text{PPh}_3)_2\text{D}$ (1- d),^{32a} $\text{CpRu}(\text{dpmp})\text{Cl}$, $\text{CpRu}(\text{dppe})\text{Cl}$,^{32b} $\text{CpRu}(\text{dpmp})\text{H}$ (2), $\text{CpRu}(\text{dppe})\text{H}$ (3),^{32c} $\text{CpRu}(\text{dppp})(\text{H})_2^+\text{BF}_4^-$,^{32d} and $\text{Cp}_2\text{Fe}^+\text{PF}_6^-$ ^{32e} were prepared according to published procedures. $\text{CpRu}(\text{dppp})\text{Cl}$ was prepared following a procedure analogous to that described for the dppe and dpmp chlorides.^{32b} Other chemicals were used as received from commercial suppliers. The oxidation of $\text{CpRu}(\text{PPh}_3)_2\text{H}$ with $\text{Cp}_2\text{Fe}^+\text{PF}_6^-$ has been previously described.^{6d}

$\text{CpRu}(\text{dppp})\text{H}$ (4). This complex has been previously synthesized,^{2b,32d} but the detailed procedure apparently has not been given. A solution of NaOMe was prepared by adding sodium metal (207 mg, 9.00 mmol) to dry methanol (35 mL) at 0°C . $\text{CpRu}(\text{dppp})\text{Cl}$ (420 mg, 0.684 mmol) was added, and the solution was heated at reflux until the solution turned yellow, ca. 45 min. The mixture was concentrated to 10 mL, and water was added to precipitate the product as yellow microcrystals. The crystals were isolated by filtration and washed with cold (0°C) methanol. The product was then washed with cold pentane and dried under vacuum (298

(31) (a) Ahlberg, E.; Parker, V. D. *J. Electroanal. Chem. Interfacial Electrochem.* **1981**, *121*, 57. (b) Ahlberg, E.; Parker, V. D. *Acta Chem. Scand., Ser. B* **1980**, *B34*, 97.

(32) (a) Wilczewski, T.; Bochenska, M.; Biernat, J. F. *J. Organomet. Chem.* **1981**, *215*, 87. (b) Ashby, G. S.; Bruce, M. I.; Tomkins, I. B.; Wallis, R. C. *Aust. J. Chem.* **1979**, *32*, 1003. (c) Bruce, M. I.; Humphrey, M. G.; Swincer, A. G.; Wallis, R. C. *Aust. J. Chem.* **1984**, *37*, 1747. (d) Conroy-Lewis, F. M.; Simpson, S. J. *J. Chem. Soc., Chem. Commun.* **1987**, 1675. (e) Lyatfov, I. R.; Solodovnikov, S. P.; Babin, V. N.; Materikova, R. B. *Z. Naturforsch., B* **1979**, *34B*, 863.

(33) (a) Walker, N.; Stuart, D. *Acta Crystallogr., Sect. A* **1983**, *A39*, 158. (b) Gilmore, C. J. *J. Appl. Crystallogr.* **1984**, *17*, 42. (c) Mallinson, P. R.; Muir, K. W. *J. Appl. Crystallogr.* **1985**, *18*, 51.

(27) (a) Tyler, D. R. *Acc. Chem. Res.* **1991**, *24*, 325. (b) Trogler, W. C. In *Organometallic Radical Processes*; Trogler, W. C., Ed.; Elsevier: New York, 1990; p 306. (c) Tyler, D. R., ref 27b, p 338.

(28) Skagestad, V.; Tilset, M. *Organometallics* **1991**, *10*, 2110.

(29) (a) Hamon, P.; Hamon, J.-R.; Lapinte, C. *J. Chem. Soc., Chem. Commun.* **1992**, 1602. (b) Hamon, P.; Toupet, L.; Hamon, J.-R.; Lapinte, C. *Organometallics* **1992**, *11*, 1429.

(30) Philbin, C. E.; Granatir, C. A.; Tyler, D. R. *Inorg. Chem.* **1986**, *25*, 4806.

mg, 75%): ^1H NMR (200 MHz, benzene- d_6) δ -12.77 (t, J = 35 Hz), 1.38 (m, 2 H), 1.81 (m, 2 H), 2.45 (m, 2 H), 4.68 (s, 5 H), 7.0–7.6 (m, 20 H).

CpRu(dppp)D (4-d). The deuteride was prepared following a procedure identical to that described for the hydride, except that methanol- d_4 was used instead of methanol. The ^1H NMR spectrum showed no detectable hydride resonance.

Oxidation of CpRu(dppm)H with $\text{Cp}_2\text{Fe}^+\text{PF}_6^-$ in Acetonitrile- d_3 . An NMR tube equipped with a ground-glass joint was charged with CpRu(dppm)H (10.0 mg, 0.018 mmol) and $\text{Cp}_2\text{Fe}^+\text{PF}_6^-$ (6.0 mg, 0.018 mmol). The tube was attached to the vacuum line and cooled with liquid nitrogen, and acetonitrile- d_3 (0.5 mL) was added by vacuum transfer. The tube was sealed under vacuum. The ^1H NMR spectrum (300 MHz) was recorded at -45°C and revealed the presence of two products: CpRu(dppm)(H_2) $^+$ (50%, δ 5.36 (s), -7.4 (br s)) and CpRu(dppm)-(NCCD $_3$) $^+$ (50%, δ 4.85 (s)).

Oxidation of CpRu(dppe)H with $\text{Cp}_2\text{Fe}^+\text{PF}_6^-$ in Acetonitrile- d_3 . A mixture of CpRu(dppe)H (10 mg, 0.018 mmol) and $\text{Cp}_2\text{Fe}^+\text{PF}_6^-$ (5.8 mg, 0.018 mmol) was added to an NMR tube equipped with a ground-glass joint. Acetonitrile- d_3 (0.5 mL) was added by vacuum transfer, and the tube was sealed under vacuum. Immediate recording of an ^1H NMR (300 MHz) spectrum at -45°C revealed the presence of three products: CpRu(dppe)(H_2) $^+$ (36%, δ 5.59 (s), -8.89 (t, J = 28.7 Hz)), CpRu(dppe)(H_2) $^+$ (9%, δ 4.95 (s), -9.25 (br s)), and CpRu(dppe)(NCCD $_3$) $^+$ (55%, δ 4.70 (s)).

Oxidation of CpRu(dppp)H with $\text{Cp}_2\text{Fe}^+\text{PF}_6^-$ in Acetonitrile- d_3 . A mixture of CpRu(dppp)H (10 mg, 0.017 mmol) and $\text{Cp}_2\text{Fe}^+\text{PF}_6^-$ (5.4 mg, 0.016 mmol) was added to an NMR tube equipped with a ground-glass joint. Acetonitrile- d_3 (0.5 mL) was added by vacuum transfer, and the tube was sealed under vacuum. Immediate recording of an ^1H NMR (200 MHz) spectrum at ambient temperature revealed the presence of two products: CpRu(dppp)(H_2) $^+$ (42%, δ 5.16 (s), -8.69 (t, J = 28.5 Hz)) and CpRu(dppp)(NCCD $_3$) $^+$ (59%, δ 4.67 (s)).

Constant-Current Coulometry. The constant-current coulometry measurement were performed in an H-shaped cell, the compartments of which were separated by a medium-frit glass junction. A platinum-gauze working electrode was used. Solutions of the hydrides (1–2 mM) in 20 mL of 1:4 THF/acetonitrile with 0.1 M Bu $_4\text{N}^+\text{PF}_6^-$ as the supporting electrolyte were electrolyzed with a constant current of 10 mA, while the consumption of the substrate was monitored by DCV. Three separate measurements were carried out for each substrate. The results are shown in Table I.

Test for H/D Exchange under Electrochemistry Conditions. Solutions of 1- d or 4- d in 10 mL of 1:4 THF/acetonitrile containing 0.1 M Bu $_4\text{N}^+\text{PF}_6^-$ were prepared. After 1 h, twice the duration of the typical electrochemical experiments, the electrolyte was concentrated to ca. a 1-mL volume by vacuum transfer. The electrolyte was precipitated by the addition of ether (20 mL), and the solution was filtered (fine porosity glass frit). The solvent was removed in vacuo, and the yellow solid was dissolved in acetonitrile- d_3 and analyzed by ^1H NMR spectroscopy. There was no evidence (<5%) for the replacement of deuterium by protons in the spectrum of 1- d ; for 4- d , some H/D exchange (<30%) had occurred.

X-ray Crystallographic Determination and Refinement of CpRu(PPh $_3$) $_2$ H (1). Crystals of 1 were obtained by diffusion of pentane vapors into a

Table V. Crystallographic Data

formula	C $_{41}$ H $_{36}$ P $_2$ Ru
fw	691.75
crystal system	triclinic
space group	P $\bar{1}$
a	9.736(1) Å
b	10.117(1) Å
c	17.659(3) Å
α	90.19(1) $^\circ$
β	105.93(1) $^\circ$
γ	99.19(1) $^\circ$
Z	2
d_{calc}	1.394 g/cm 3
size	0.6 \times 0.3 \times 0.25 mm 3
μ (Mo K α)	5.89 cm $^{-1}$
diffractometer	Nicolet P3/F
radiation	Mo K α (λ = 0.71069 Å)
temperature	138 K
scan mode	$\omega/2\theta$
2θ range	3–65 $^\circ$
no. of reflns measd total	9543
no. of obsns $I > 3.0\sigma(I)$	7988
max peak in final diff map	1.22 e/Å 3 (0.98 Å from Ru1)
min peak in final diff map	-1.18 e/Å 3 (0.76 Å from Ru1)
structure soln	direct methods
refinement	block diagonal least squares
quantity minimized	$\sum w(F_o - F_c)^2$
weighting scheme	$w = 1/(\sigma^2(F) + 0.0003F^2)$
R	0.041 (0.049 without absorption correction)
R_w	0.047 (0.058 without absorption correction)
data/parameter	14.8

benzene solution of 1 at ambient temperature. A crystal was mounted on a glass fiber and placed in a cold N $_2$ stream. Intensity data were obtained with graphite-monochromated Mo K α radiation on a Nicolet P3/F diffractometer. Unit-cell dimensions were based upon 25 well-centered reflections ($28^\circ < 2\theta < 37^\circ$). Empirical absorption corrections were applied to the data set. 29a The structure was determined using direct methods (MITHRIL 29b), and refinements were carried out using the GX Crystallographic Program System. 29c A summary of crystal structure data is given in Table V.

Acknowledgment. This work was supported by Statoil under the VISTA program, administered by the Norwegian Academy of Science and Letters (stipend to K.T.S.), and by the Norwegian Council for Science and the Humanities (NAVF).

Supplementary Material Available: Tables of positional and thermal parameters, bond lengths, bond angles, and torsion angles (12 pages); listing of observed and calculated structure factor amplitudes for 1 (45 pages). Ordering information is given on any current masthead page.